

Probabilistic Risk Evaluation of RC Building - Comparison of Modeling Approaches.

VIMAL CHAUDHARY, K. S. BABU NARAYAN

Department of Civil Engineering, National Institute of Technology Karnataka, Surathkal, India

Email: bittujaan08@gmail.com, shrilalisuta@gmail.com

Abstract: Seismic provisions have several parameters which can be utilized to improve the performance of the structures under seismic excitations. Many studies have shown that the damage index of a structure can be decreased by changing these parameters. However, the behavior of structures subjected to earthquake excitations is probabilistic rather than deterministic. Moreover, the origin of earthquakes, the inherency of earthquakes caused by fault movement, is stochastic as well. This uncertainty is in the whole property of earthquake records, such as PGA and frequency content. The evaluation of structures cannot be concluded if all these uncertainties are neglected. In addition, there is no sufficient guarantee that considering such parameters, which are definitely introduced in seismic provisions, improves the performance of structures and operates very precisely. A decrease in damage index does not mean that the probability of damage exceedance and loss estimation can be declined. Moreover, the origin of earthquakes, the inherency of earthquakes caused by fault movement, is stochastic as well. Hence, the uncertainty is in the whole property of earthquake records, such as peak ground acceleration and frequency content. Vulnerability and risk assessment can be evaluated in a deterministic or a probabilistic way and this study makes a comparison between the two modeling approaches based on the capacity spectrum method procedures. Comparison of fragility curves developed using different procedures is studied and applicability is discussed. Seismic fragility curves were developed and damage probability indices has been constructed for the chosen example problems.

Keyword: Mander Method, Moment-Curvature, Modified Kent & Park Method, Fragility Curve, Damage Index

1. Introduction:

Since the country lie in earthquake prone area and many of the destructive earthquakes occurred in the history so far resulting in high number of casualties due to collapse of buildings and dwellings. A major challenge for the performance based seismic engineering is to develop simple yet efficiently accurate methods for analyzing designed structures and evaluating existing buildings to meet the selected performance objectives. Elastic analyses are insufficient because they cannot realistically predict the force and deformation distributions after the initiation of damage in the building. Inelastic analytical procedures become necessary to identify the modes of failure and the potential for progressive collapse. The need to perform some form of inelastic analysis is already incorporated in many building codes. Theoretical moment-curvature analysis for reinforced concrete columns, indicating the available flexural strength and ductility, can be conducted providing the stress-strain relation for the concrete and steel are known. The moments and curvatures associated with increasing flexural deformations of the column may be computed for various column axial loads by incrementing the curvature and satisfying the requirements of strain compatibility and equilibrium of forces.

2. Stress-Strain Models for confined concrete:

Failure of reinforced concrete structures can be categorized by material failure, mechanical failure or combination between material and mechanical failure. Unlike the simple approach used for analyzing the behavior of plain concrete, the more complicated

analysis of confined concrete has been conducted for about a hundred years and many models have been proposed. The mother source equation for most of the models is having the form $f_{cc} = f'_c + kf_l$ Where the maximum confined strength f_{cc} is related to the peak unconfined strength f'_c and the effective lateral confined pressure f_l with a coefficient k . This coefficient varies based on the concrete mix and the lateral confinement pressure and it was derived or obtained from the analytical and experimental work.

2.1 Kent and Park Model:

In 1971, **Kent and Park Model**, proposed a stress-strain curve for concrete confined by rectangular hoops. The suggested relationship combines many of the features of previously proposed curves. A second-degree parabola represents the ascending part of curve and assumes that the confining steel has no effect on the shape of this part of curve or the strain at maximum stress. This essentially means that the ascending curve is exactly the same for both confined and unconfined concrete. It is also assumed that the maximum stress reached by confined concrete is equal to the cylinder strength f'_c that is reached at a strain of 0.002

In 1982, a modified form of Kent and Park model was proposed. This model makes an allowance for the enhancement in the concrete strength due to confinement. Figure-2 shows the modified Kent and Park model.

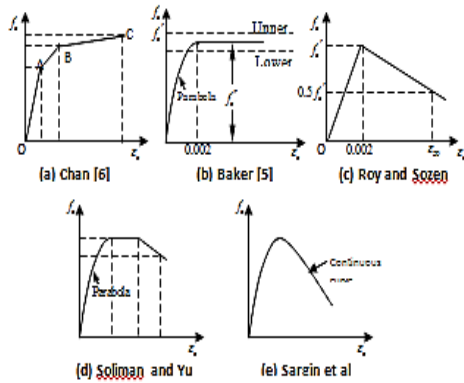


Figure 1 Proposed Stress-strain curves for concrete confined by rectangular hoops

The maximum stress reached (at point B) is assumed to be Kf'_c at a strain of $\epsilon_0 = 0.002K$, in which,

$$K = 1 + \frac{\rho_s f_{yh}}{f'_c}$$

f_{yh} = yield strength of steel hoops.

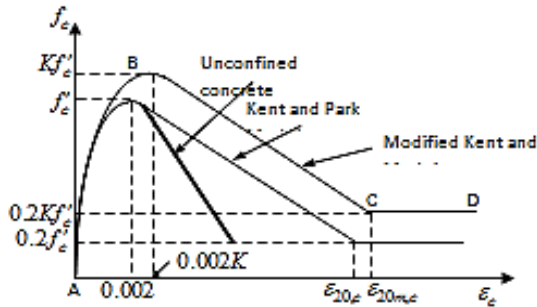


Figure 2 Modified Kent and Park Stress-strain curve for confined concrete

ρ_s = Ratio of volume of transverse reinforcement to volume of concrete core measured to outside of hoops.

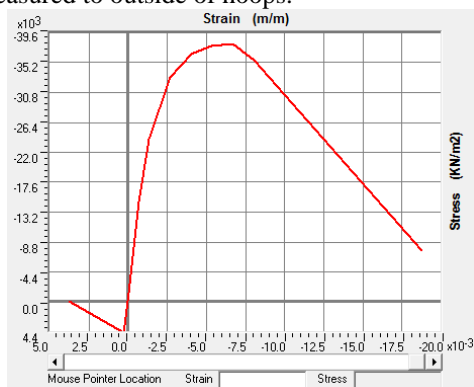


Figure 3 Modified Kent and Park Stress-strain curve input in software SAP2000

2.2 Mander's model:

Mander's model is another highly popular model since it is simple and effective in considering the effects of confinement. He first tested circular, rectangular and square full scale columns at seismic strain rates to investigate the influence of different

transverse reinforcement arrangements on the confinement effectiveness and overall performance. Mander (1988) went on to model their experimental results. It was observed that if the peak strain and stress coordinates could be found (ϵ_{cc} , f'_{cc}) then the performance over the entire stress-strain range was similar, regardless of the arrangement of the confinement reinforcement used.

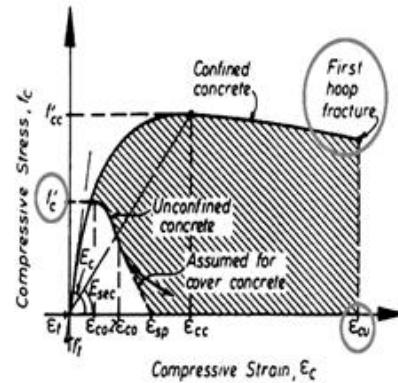


Figure 4 Mander Model for Stress-Strain

This model is discussed in detail and is used for this project. This model is popularly used to evaluate the effective strength of the columns confined by stirrups, steel jacket and even by FRP wrapping. Mander's model does not handle the post-peak branch of high strength concrete particularly well and requires some modification.

The effective cylinder strength of the confined concrete f_{cc} , which is equal to 0.8 times the cube strength of the confined concrete, is given by,

$$f_{cc} = f'_c \left(-1.254 + 2.254 \sqrt{1 + \frac{7.94f'_l}{f'_c} + \frac{2f'_l}{f'_c}} \right)$$

Where,

f'_c = The cylinder strength of unconfined concrete = $0.8f_{ck}$

f_{cc} = The cylinder strength of confined concrete

f'_l = the confining stress

$$f'_l = (1/2) k_e \rho_s f_{yh}$$

In which ρ_s = ratio of volume of transverse confining steel to volume of confined concrete core, f_{yh} = yield strength of transverse reinforcement, k_e = confinement coefficient.

The stress in concrete (f_c), corresponding to a strain (ϵ_c) is given by

$$f_c = \frac{f'_{cc} x r}{r - 1 + x^r}$$

Where,

$$x = \frac{\epsilon_c}{\epsilon_{cc}}$$

$$\epsilon_{cc} = 0.002 \left[1 + 5 \left(\frac{f'_{cc}}{f'_c} - 1 \right) \right]$$

$$r = \frac{E_c}{E_c - E_{sec}}$$

$$E_c = 5000\sqrt{f'_c} \text{ (MPa)}$$

$$E_{sec} = \frac{f'_{cc}}{\epsilon_{cc}}$$

$$E_{sec} = \frac{f'_c}{\epsilon_{cc}}$$

The maximum transverse pressure from the confining steel can only be exerted effectively on that part of the concrete core where the confining stress has fully developed due to arching action. Figure 5 shows the arching action that is assumed to occur between the levels of transverse circular and rectangular hoop reinforcement. Midway between the levels of the transverse reinforcement, the area of ineffectively confined concrete will be largest and the area of effectively confined concrete core A_e will be smallest.

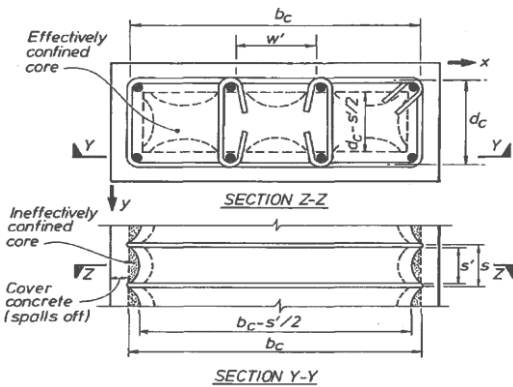


Figure 5 Section showing the arching action in Rectangular hoops

The arching action Figure 5 is again assumed to act in the form of second-degree parabolas with an initial tangent slope of 45° . Arching occurs vertically between layers of transverse hoop bars and horizontally between longitudinal bars. The effectively confined area of concrete at hoop level is found by subtracting the area of the parabolas containing the ineffectively confined concrete. For one parabola, the ineffectual area is $(w_i'/2)^2/6$, where w_i' is the i^{th} clear distance between adjacent longitudinal bars (see Figure 3.7). Thus the total plan area of ineffectually confined core concrete at the level of the hoops when there are n longitudinal bars is

$$A_i = \sum_{i=1}^n \frac{(w_i')^2}{6}$$

Incorporating the influence of the ineffective areas in the elevation, the area of effectively confined concrete core at midway between the levels of transverse hoop reinforcement is

$$A_e = \left(b_c d_c - \sum_{i=1}^n \frac{(w_i')^2}{6} \right) \left(1 - \frac{(s)'}{2b_c} \right) \left(1 - \frac{(s)'}{2d_c} \right)$$

Where b_c and d_c = core dimensions to centrelines of perimeter hoop in x and y directions, s = centre to centre distance between stirrups, and s' = clear distance between stirrups, where $b_c > d_c$.

$$K_e = \frac{\left(1 - \sum_{i=1}^n \frac{(w_i')^2}{6b_c d_c} \right) \left(1 - \frac{(s)'}{2b_c} \right) \left(1 - \frac{(s)'}{2d_c} \right)}{(1 - \rho_{cc})}$$

It is possible for rectangular reinforced concrete members to have different quantities of transverse confining steel in the x and y directions. These may be expressed as,

$$\rho_x = \frac{A_{sx}}{s d_c} \quad \rho_y = \frac{A_{sy}}{s b_c}$$

Where A_{sx} and A_{sy} = the total area of transverse bars running in the x & y directions, respectively, Figure 5 The effective lateral confining stresses in x and y directions are:

$$f'l_x = k_e \rho_x f_{yh} \text{ and } f'l_y = k_e \rho_y f_{yh}$$

Therefore, $f'l = f'l_x + f'l_y$

The ultimate strain in concrete is given by the equation

$$\epsilon_{cu} = 0.004 + \frac{1.4 \rho_s f_{yh} \epsilon_{sm}}{f'_{cc}}$$

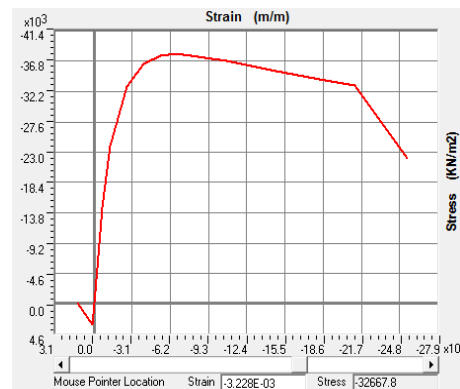


Figure 6 Mander's Stress-strain curve input in software SAP2000

2.3 Stress-strain models for reinforcing steel:

The idealized stress-strain curve for steel as recommended by IS: 456-2000 is as shown in British code CP 110-1972 as in Figure 7, it says that the term $0.7f_y$ is the simplification of the expression $\left[\frac{f_y}{\gamma_m + \frac{f_y}{2000}} \right]$.

It gives all the simplified general equations which can be used for any grade of steel.

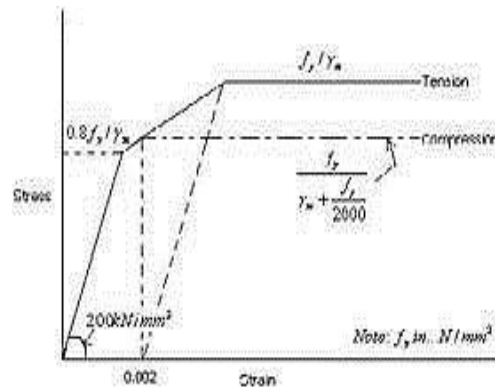


Figure 7 stress-strain curve for steel

3 Structural Systems:

The building is an RC G+3 framed structure. The floor plan is same for all floors. The beam arrangement is different for the roof. It is symmetric in both the direction. The concrete slab is 120 mm thick at each floor level.

Overall geometry of the structure including the beam layout of all the floors is as shown in Figure below.

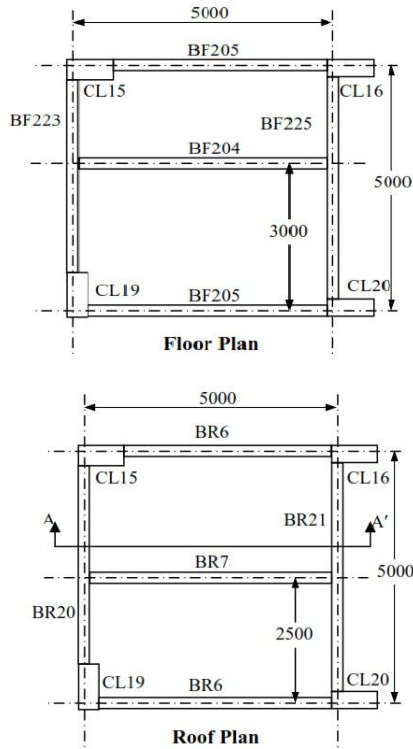


Figure 8 Floor and Roof Plan of the structure

Table below shows the size and reinforcement details for beam sections at the Column face.

3.1 Dynamic Properties of Building:

Structure used for analysis is a four storied RCC structure with single bay 5m x 5m dimension. Height of the storey is 4m. The structure is modeled in SAP2000 and the dynamic properties of the building is calculated and presented in Table 2, based on that the lateral loads are calculated and the structure is then analyzed by applying the lateral loads.

Time period and mode shapes are two of the most important dynamic properties of building. These are the pre-requisite parameters for the analysis and design of buildings for random type load like earthquakes. Response of a building to dynamic loads depends primarily on the characteristics of both the excitation force and the natural dynamic properties of the building. These properties can be computed both analytically and experimentally. Figure-10 shows the normalized mode shapes of the building.

Table: 1 Reinforcement details of beam section

Beam	Size (mm)	Length (m)	Longitudinal Reinforcement		Transverse Reinforcement
			Top	Bottom	
BF 204	230 x 1000	5	2#16	3#16	2#8@200 c/c
BF 205	230 x 1000	5	2#25	2#25	2#10@125 c/c
BF 223	230 x 1000	5	2#25	2#25, 1#16	2#10@125 c/c
BF 225	230 x 1000	5	2#20	2#25	2#10@150 c/c
BR 6	230 x 1000	5	2#20	3#20	2#8@200 c/c
BR 7	230 x 600	5	2#16	3#16	2#8@120 c/c
BR 20	230 x 1000	5	2#20	2#25	2#8@175 c/c
BR 21	230 x 1000	5	2#20	2#20	2#8@175 c/c

Note: # represents Torsteel

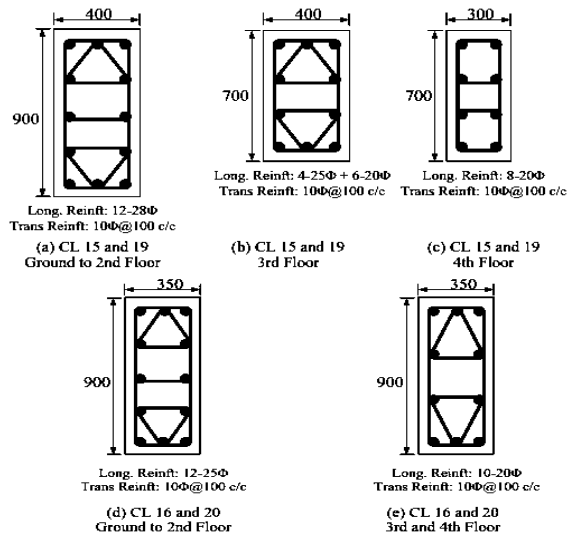


Figure 9 Details of columns at various levels

Table: 2 Dynamic Properties of the Building

Modal Properties	Mode	
	1	2
Period (sec)	0.469	0.356
Modal Participation Factor	229.91	150.62
Modal Mass ratio	0.0048	0.695

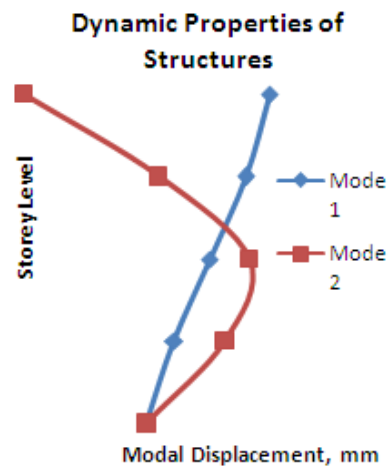


Figure-10 Normalized Mode Shape of the Structure

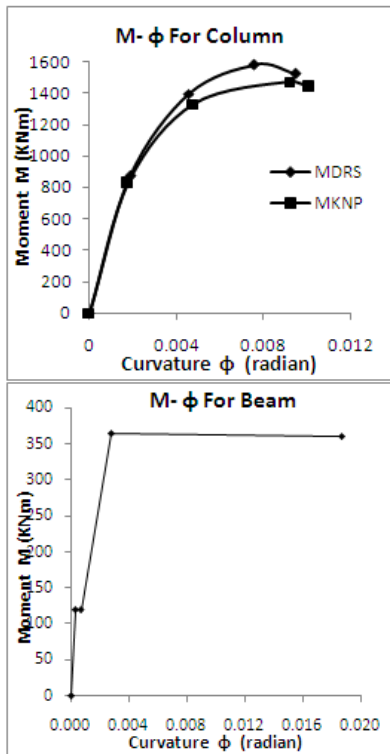


Figure 11 -Moment-curvature relationship curve for column and beam

Table –3 Moment at various points in Column

Column	Origin	Yield	Ultimate	Strain hardening	Strain hardening	
CL 15/19 G/2nd	MDRS	0	987.64	1579.79	802.36	807.57
	MKNP	0	827.92	1328.44	811.6	803.71
CL 15/19 3rd	MDRS	0	440.52	673.07	228.49	230.42
	MKNP	0	488.17	559.23	226.57	231.12
CL 15/19 4th	MDRS	0	272.34	406.21	219.88	221
	MKNP	0	319.09	314.76	164.64	169.45
CL16/20 G/2nd	MDRS	0	792.81	1215.82	647.9	652.28
	MKNP	0	918.25	1014.34	293.73	293.73
CL 16/20 3/4th	MDRS	0	469.46	723.76	295.62	305.88
	MKNP	0	527.14	581.94	261.87	266.85

The figure below show the moment – curvature relationship as generated by the SAP2000 for 50% of axial load capacity and given as input for the non-liner property of the member. Here MDRS stand for Mendar’s modeling and MKNP stand for modified Kent and Park method of modeling

4 Probabilistic Risk Analyses:

The study provide an analytical methodology to quantify hazard through system reliability for the probabilistic risk analysis of reference building as depicted in Figure 8,

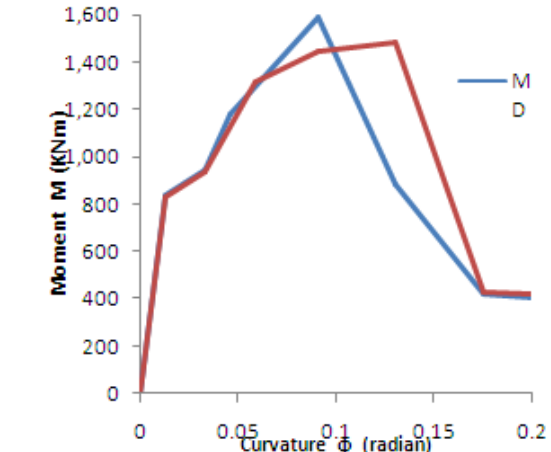


Figure-12 Moment-curvature relationship curve for column for MKNP and MDRS

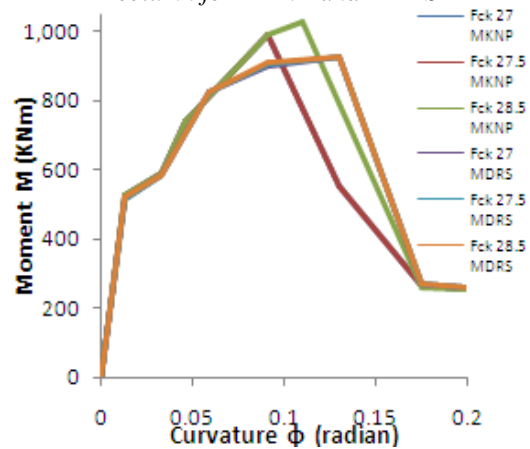


Figure -13 Moment-curvature relationship curve for column for MKNP and MDRS for different values of Fck

Vulnerability and risk assessment can be evaluated in a deterministic or a probabilistic way starting from the capacity curve obtained with a static non-linear analysis, fragility curves were plotted and an average damage index for the performance point of the structure was calculated. In the probabilistic approach the influence of uncertainties in the damage states thresholds is investigated on fragility and vulnerability curves.

4.1 Simplified Non-linear Analysis Procedure:

The two key points of a performance based design procedure are demand and capacity. Demand is the representation of the earthquake ground motion. Capacity is representation of the structure’s ability to resist the seismic demand. The performance is dependent on the manner that the capacity is able to handle the demand. In other words, the structure must have the capacity to resist the demand of the earthquake such that the performance of the structure is compatible with the objectives of the design. Simplified nonlinear analysis procedure using pushover methods, require determination of three primary elements

- a) Capacity,
- b) Demand (displacement), and
- c) Performance.

Capacity:

The overall capacity of the structure depends on the strength and deformation capacities of the individual components of the structure. In order to determine capacities beyond the elastic limits, some form of nonlinear analysis such as the pushover procedure, is required. In this procedure, at first the load is applied to the mathematical model of the structure and is allowed to increase in the same ratio till some member(s) fail. The mathematical model of the structure is then modified with zero or very small stiffness for the yielding elements (hinge formation). The load is again increased to this new modified model until some other elements yield. This procedure is repeated till the structure reaches an ultimate limit, such as instability from P-Delta effects; distortions considerably beyond the desired the performance level; an element (or group of elements) reaching a lateral deformation level at which significant strength degradation begins; or an element (or group of elements) reaching a lateral deformation level at which loss of gravity load carrying capacity occurs. Therefore we can say that, this procedure uses a series of sequential elastic analyses, superimposed to approximate a force displacement capacity diagram of the overall structure.

Demand:

Demand is a representation of the earthquake ground motion or shaking that the building is subjected to. In nonlinear static analysis procedures, demand is represented by an estimation of the displacements or deformations that the structure is expected to undergo. This is in contrast to conventional, linear elastic analysis procedure in which demand is represented by prescribed lateral forces applied to the structure. Ground motion during an earthquake produces complex horizontal acceleration and therefore displacement patterns in structures that may vary with time. Tracking these motions at every time step to determine structural design requirement is judged impractical. Traditional linear analysis methods use lateral forces to represent a design condition. For nonlinear method it is easier to use a set of lateral displacements as a design condition. For a given structure and ground motion, the displacement demand is an estimate of the maximum expected response of the building during the ground motion.

Performance:

Once capacity curve and demand displacements are defined, a performance check can be done. A performance check verifies that structural and non-structural components are not damaged beyond the acceptable limits (strength or serviceability limits) of the performance objective for the forces and displacement implied by the displacement demand. A performance objective specifies the desired seismic performance of the building. It is a desired level of seismic performance of the building; i.e., a limiting damage state within the building, the threat to life

safety of the building's occupants due to the damage, and the post-earthquake serviceability of the building; generally described by specifying the maximum allowable (or acceptable) structural and non-structural damage, for a specified level of seismic hazard.

4.2 Evaluation of performance capacity:

Performance point is considered as a point where demand and capacity curve intersects with each other. Performance evaluation is the main objective of a performance based design. A component or action is considered satisfactory if it meets a prescribed performance. The main output of a pushover analysis is in terms of demand versus capacity. If the demand curve intersects the capacity envelope near the elastic range, Figure-14a, then the structure has a good resistance. If the demand curve intersects the capacity curve with little reserve of strength and deformation capacity, Figure. 14b, then it can be concluded that the structure will behave poorly during the imposed seismic excitation and need to be retrofitted to avoid future major damage or collapse.

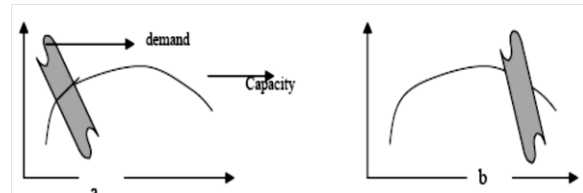


Figure 14 Typical seismic demand versus capacity (a) safe design; (b) unsafe design

Nonlinear Static Pushover (NSP) analysis, which is basically an inelastic static analysis procedure that gives due consideration to the material non-linearity, is an effective and efficient tool to evaluate the performance of the structure under lateral loads especially seismic loads. The method not only provides information on strength capacity of the structures but also provides vital information on ductility as well as an insight on the progressive mode of failure of the structure. Thus the method is more performance-based than being conventional strength-based approach

4.3 Non-linear Dynamic Analysis (Time History Analysis):

Conventional time History Analysis is carried out to determine the ground motion intensity the building must be subjected to for it to displace to a specified inter-story drift ratio using SAP/E-TABS software's of latest version. The general procedure for the implementation of the probabilistic Capacity Spectrum Method (CSM) is as shown in Figure.

Eleven ground motions are to be selected such that variability of ground that significantly affects the elastic and inelastic response of the existing RC buildings under consideration should be effectively be captured. Most of the methods proposed for selection of recorded earthquake ground motions for time-history analysis focus on matching the response spectra of selected ground motions with the given

design spectra. However, the seismic design spectra in the seismic codes represent an average value from statistics. A final set of 11 time histories was selected, which simultaneously satisfies the largest lognormal dispersion in spectral acceleration scaled/unit PGA and least lognormal dispersion in inelastic displacement when records are scaled to median S_a for T_n in the range 0.6–1.0 s. In this According to the empirical findings by Sewell, the linear response of SDOF system is independent of M and R . Shome and Cornell have later shown that scaling is not a bias for the multi-degree-of-freedom (MDOF) systems and proper scaling can reduce dispersion of response to one-fourth that of actual dispersion.

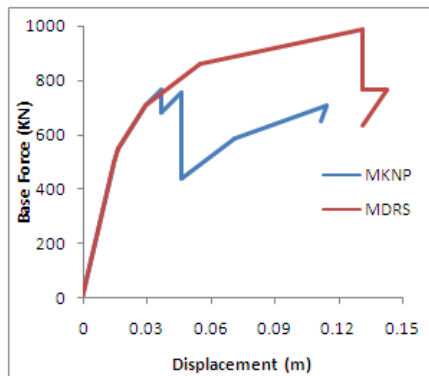


Figure 15 Analytical pushover curve of building by MKNP and MDRS modelling.

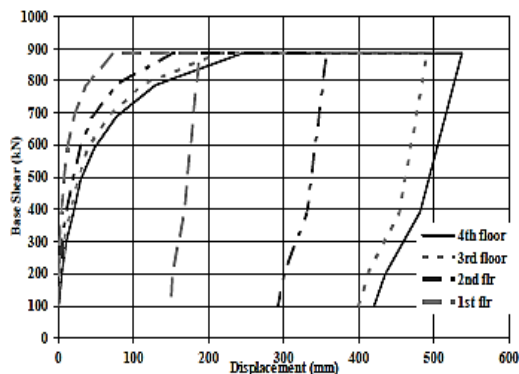


Figure 16 Experimental pushover curve of building.

All selected ground motions have been uniformly scaled to 1 m/s² (unit) PGA and applied to the linear and nonlinear SDOF systems having natural period ranging from 0.6 to 1.0 s to evaluate various ground-motion parameters.

4.4 Ground-motion parameters:

Since the first strong ground motion was recorded in 1933, a large number of strong ground motions have been recorded in the world. On the basis of these ground motions, researchers have proposed different parameters to characterize the ground-motion damage potential.

These parameters range from a simple instrumental peak value to that resulting from a complicated mathematical derivation. Ground-motion parameters are essential for describing the important

characteristics of strong ground motion in compact, quantitative form. Many parameters have been proposed to characterize the amplitude, frequency content and duration of strong ground motions; some describe only one of these characteristics, while others may reflect two or three. Because of the complexity of earthquake ground motions, identification of a single parameter that accurately describes all important ground-motion characteristics is not possible. Various significant engineering parameters have been evaluated and detailed statistical study has been carried out on parameters calculated for the 11 time histories selected. Suitability of various ground-motion parameters as IM has been discussed and conclusions have been drawn. Modified parameters have also been defined.

Table –3 Available Indian strong motion records

SL	Earthquake Event	Date	Magnitude (Mw)	Station	R (Km)	Peak Acceleration
1	Bhuj Earthquake	26-Jan-01	7	Ahmedabad	239	0.78236
2	India-Bhutan	21-Sep-09	6.2	Cooch Vihar		0.15656
3	Chamoli (Nw Himalaya) Earthquake	29-Mar-99	6.6	Gopeshwar	17.3	1.9507
4	Myanmar-India(Manipur)-Border	29-Dec-09	5.5	Guwahati		0.10919
5	N.E. India Earthquake	6-May-95	6.4	Diphu	245.6	1.003
6	N.E. India Earthquake	8-May-97	5.7	Jellaipur	41.9	1.1519
7	Ne-India Earthquake	6-Feb-88	5.8	Dauki	80.5	0.379
8	Ne-India Earthquake	6-Aug-88	7.2	Bokajan	189.9	2.2
9	Ne-India Earthquake	18-May-87	5.9	Laisong	102.3	0.601
10	Off-Coast-Of-Nicobar	6-Dec-10	6.3	Por		0.04739
11	Uttarkashi Earthquake	19-Oct-91	7	Bhatwari	21.7	2.42

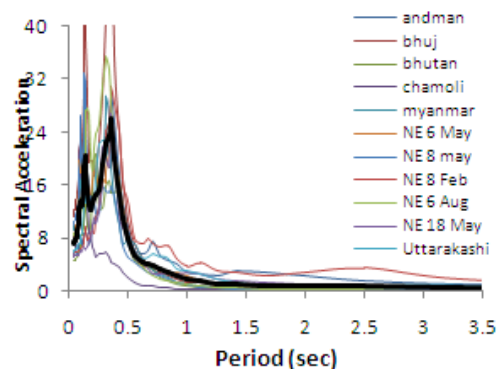


Figure 17 Response spectra of the selected ground motions by MKNP modeling.

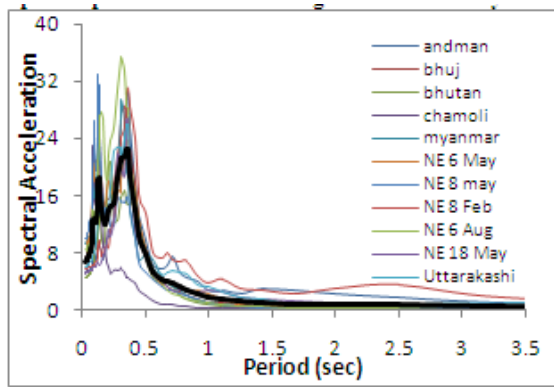


Figure 18 Response spectra of the selected ground motions by MDRS modeling,

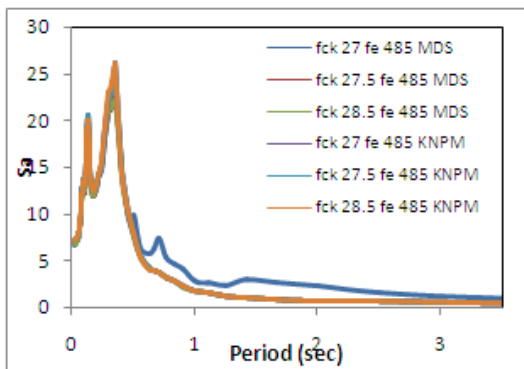


Figure 19 Average Response spectra of the selected ground motions by MKNP and MDRS for different Fck values,

4.5 Define Damage State Indicator Levels (Failure Criteria and Performance Limit States):

The top storey displacement is often used by many researchers as a failure criterion because of the simplicity and convenience associated with its estimation. The limit states (immediate occupancy, life safety, and collapse prevention) associated with various performance levels of reinforced concrete frames as mentioned in FEMA 356 and the damage state indicator levels are defined depending on progressive collapse starting from yielding and rotation to instability.

One of the most challenging steps in probabilistic risk analysis is the determination of damage parameters and their corresponding limit states. These parameters are very essential for defining damage state as well as determining the performance of RC building under a seismic event. Therefore, realistic damage limit states are required in the development of reliable fragility curves, which are employed in the seismic risk assessment packages for mitigation purposes.

The considered approach proposes four damage states: slight – the damage is considered negligible, moderate – slight structural damage and moderate non-structural damage, severe – moderate structural damage and Ioana Olteanu et al. heavy non-structural damage and collapse when structure is in imminent

danger of collapse. Table 1 shows a summary of the used parameters for the damage state thresholds as functions of the yielding displacement, dy , and the ultimate displacement, du , of the structure (Milutinovic & Trendafiloski, 2003). A further step is given by describing the seismic structural damage by means of vulnerability curves. These curves are useful in risk analyses of urban areas, in which case a library of curves covering all the existing building typologies can be realized. They quantify the damage as a function of a parameter characterizing the seismic action, for example the spectral displacement, Sd . From a theoretical point of view, they represent the normalized mathematical expectation of the damage states in each spectral displacement (Sobol, 1983):

$$DI = \frac{1}{n} \sum_{i=1}^n x_i p_i$$

Where DI is the mean damage index, x_i – the damage state number which varies from 1 to 4, and p_i – the probability of corresponding damage state. The probability of damage is computed from the fragility curves.

Table: 4 Damage State Indicator Levels

Slight Damage	Hinge yielding at one floor
Moderate Damage	Yielding of beams or joints at more than one floor
Extensive Damage	Hinge rotation exceeds plastic rotation capacity
Collapse	Structural Instability

Table: 5 Damage State Thresholds

Damage state	\bar{Sd}_{ds} values	Graphical representation of the damage thresholds in the bilinear capacity spectrum
Slight	$0.7dy$	
Moderate	dy	
Severe	$dy + 0.25(du - dy)$	
Collapse	du	

Maximum roof displacements were calculated with nonlinear dynamic analyses for different accelerograms and different values of peak ground acceleration. More about mathematical model of the structure can be finding in Dollek & Fajfar (2001). Eleven accelerograms were selected from the Indian Strong-Motion Database. All accelerograms were recorded on stiff soil. Scaled acceleration spectra are presented in Figure 17 and 18. It can be observed that average spectrum of the selected group of accelerograms is similar to the IS-1893 spectrum.

Each curve represents several non-linear dynamic analyses for particular accelerograms and different values of peak ground acceleration. These motions were characterized by surface wave magnitudes, M_s , ranging from 5 to 7, and closest distances to the rupture surface.

4.6 Building Fragility Curves:

Develop an analytical fragility estimates to quantify the seismic vulnerability of RC frame building Assessment of seismic behaviour and fragility of buildings using HAZUS The probabilistic methodology for seismic evaluation of existing buildings implemented in HAZUS (*Earthquake Loss Estimation Methodology – HAZUS – Technical Manual, 1997*) assess the seismic fragility using the .capacity spectrum method. (Freeman, Nicoletti & Tyrell, 1975). The step-by-step procedure to assess the seismic fragility of existing buildings is highlighted in the following, HAZUS (1997):

In order to evaluate the building behaviour, capacity curves can be obtained through nonlinear analysis. The capacity curve is in fact the graphical representation of the relation between the base shear and the displacement at the roof of the structure. The capacity spectrum method requires the following steps: (1) perform the pushover analysis of the building; (2) plot the capacity curve of the building; (3) represent it in a ADRS format, that is, spectral displacement – spectral acceleration coordinates; (4) calculate and plot the bilinear representation of the capacity spectrum; (5) plot the demand spectrum of the considered earthquake; and finally (6) intersect capacity and demand spectra to obtain the performance point, and thus the expected spectral displacement. Even though there are a variety of methods to evaluate the behavior of the structure, it is considered that the pushover analysis is an accurate approximation in comparison with the nonlinear dynamic analysis. The performance point is calculated using the equal displacement approximation described in ATC-40.

In order to evaluate the seismic risk of a building, damage fragility curves are used. Fragility curves define the probability that the expected global damage, *d*, of a structure exceeds a given damage state, *dsi*, as a function of a parameter quantifying the severity of the seismic action. Thus, for each damage state, the corresponding fragility curve is completely defined by plotting $P[d \geq dsi]$ in the ordinate and the spectral displacement, *Sd*, in the abscissa. For a given damage state, *dsi*, a fragility curve is well described by the following lognormal probability density function (Barbat *et al.*, 2008):

$$P[dsi|Sd] = \varphi \left[\frac{1}{\beta_{dsi}} \ln \left(\frac{Sd}{Sd_{dsi}} \right) \right]$$

where *Sd* is the spectral displacement (seismic hazard parameter), representing the median value of spectral displacement at which the building reaches a certain threshold of the damage state, *dsi*, β_{dsi} – the standard deviation of the natural logarithm of the spectral displacement of the damage state *ds* and Φ – the standard normal cumulative distribution

Once the parameters of fragility function, *Sd*, *ds* and β_{ds} , are obtained one can compute and plot the functions using equation

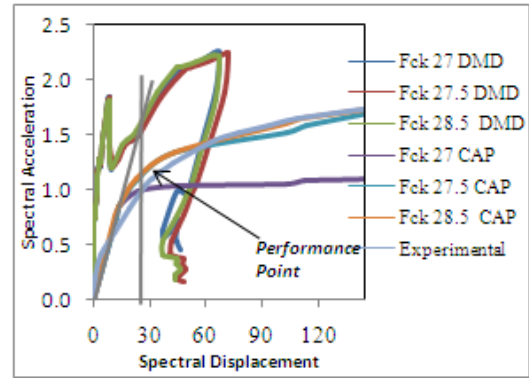


Figure 20 Evaluation of the performance point by MDRS modeling

Table 6 Performance point by MDRS

Performance Point	Fck 27	Fck 27.5	Fck 28.5	Experimental
Sa	.98	1.16	1.18	1.18
Sd	28	36	36	37

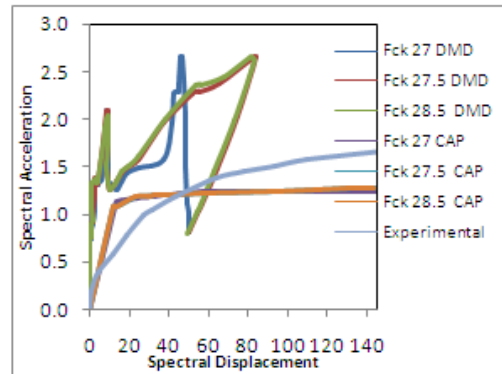


Figure 21 Evaluation of the performance point by MKNP modeling approach

Table 7 performance point by MKNP

Performance Point	Fck 27	Fck 27.5	Fck 28.5	Experimental
Sa	1.12	1.16	1.16	1.18
Sd	16	17	17	37

Here DMD stand for Demand curve and CAP stand for Capacity curve.

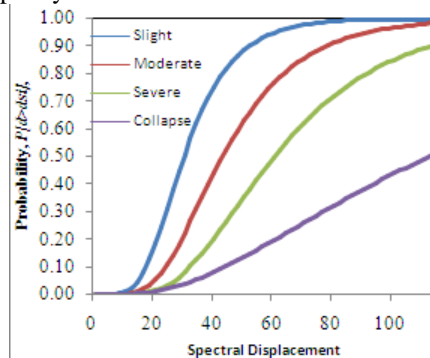


Figure –22 Fragility curves representation for Fck 27 by MDRS modeling

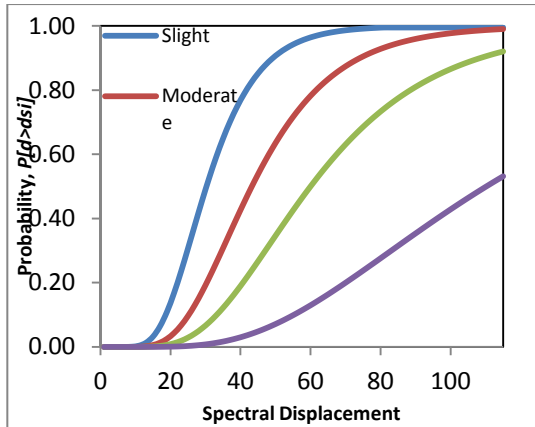


Figure –23 Fragility curves representation for Fck 27.5 by MDRS

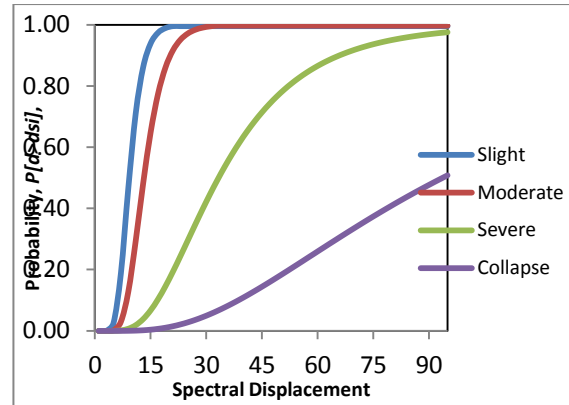


Figure –27 Fragility curves representation for Fck 28.5 by MKNP

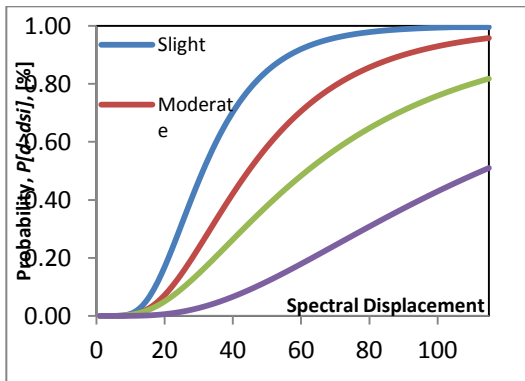


Figure-24 Fragility curves representation for Fck 28.5 by MDRS

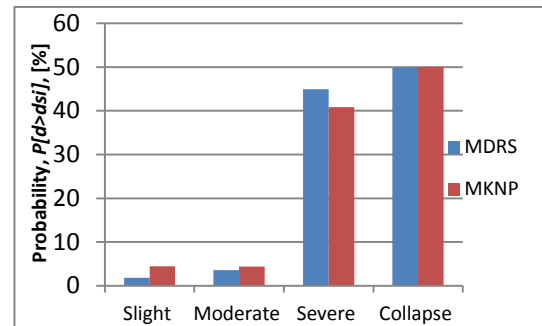


Figure –28 Damage states thresholds probabilities for Fck 27

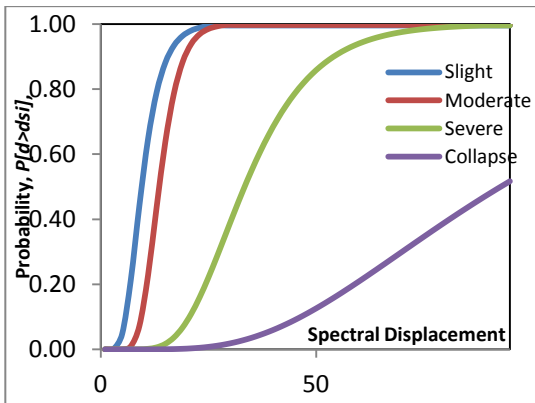


Figure –25 Fragility curves representation for Fck 27 by MKNP

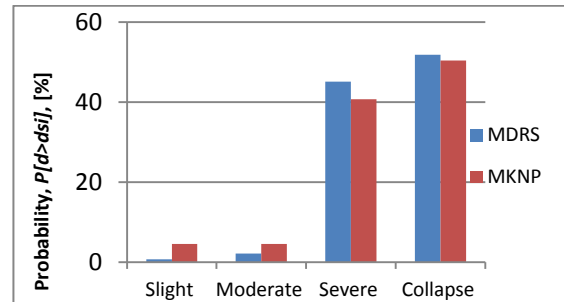


Figure –29 Damage states thresholds probabilities for Fck 27.5

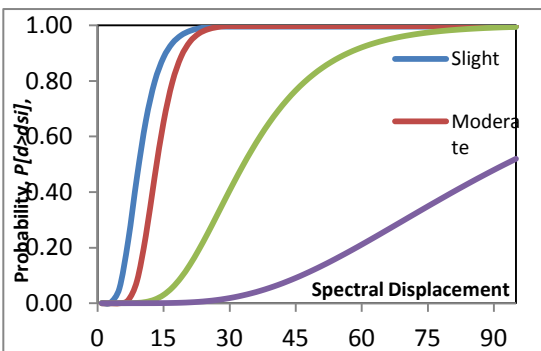


Figure –26 Fragility curves representation for Fck 27.5 by MKNP

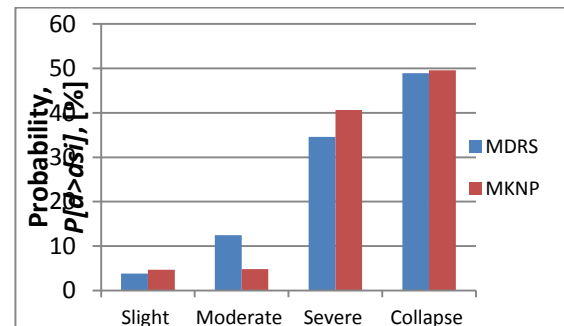


Figure –30 Damage states thresholds probabilities for Fck 28.5

5 Conclusions:

The main advantage of the probabilistic approach consists in the fact that the obtained results are closer to the real behaviour of the building that is, to the uncertainties the building can suffer during its life time.

As show in figure 15 and Figure 16 it is very clearly seen that the pushover curve obtain by MDRS modeling approach is more closer and smooth to the pushover curve obtain in experimental work.

The base shear obtain in MDRS modeling having the difference of $\pm 5\%$ which is more closer to the experimental results where as in MKNP modeling the base shear found 13% lesser as compare to experimental results.

In the moment-curvature curve Figure 11 and Figure 12 it has been observed that the yield moment are approximately same by both MDRS and MKNP modeling method but the ultimate moment in MKNP modeling is found slightly lesser than the MDRS modeling method. And the ultimate curvature in MKNP modeling is slightly more than MDRS modeling approach.

From the Figure 17 ,18 and 19 in average response spectra of all selected earth quake, the peak value of spectral acceleration in both the method are found approximately same, The average response spectra of the structure are not much affected by small variation of concrete strength. From the figure 20 and 21 the performance point in MDRS modeling is found closer to the experimental value. Similarly in the 28, 29, and 29 it is clear the probability of collapse in both the method are more or less equal in small variation of concrete strength. In overall study the results in MDRS are fount more closely to the experimental results.

References:

- [1] Bertero V.V., Uang C., 1997, "Issues and Future Directions in the Use of an Energy Approach for Seismic-Resistant Design of Structures in Nonlinear Seismic Analysis and Design of Reinforced Concrete Buildings", P. Fajfar and H. Krawinkler, Eds., Elsevier Applied Science, London and New York.
- [2] Shinozuka M, Mizutani M, Takeda M, Kai Y., 1989, "Seismic PRA Procedure in Japan and Its Application to Building Performance Safety Estimation", Part 3. Estimation of Building and Equipment Performance Safety, Proc ICOSSAR 89, 5th Int Conf on Structural Safety and Reliability, Publ by ASCE, New York, USA, 637-644.
- [3] Anand S. Arya., 2000, "Recent developments toward earthquake reduction in India", Current Science, 79(9), 1270-1277.
- [4] Choudhary M.R., Upton M and Haldar A., 2001, "Seismic reliability assessment of reinforced concrete frames under seismic loading", 8th International conference on structural safety and reliability (ICOSSAR 2001), Paper No. 237.
- [5] Krawinkler H. and Seneviratna G.D.P.K., 1998, "Pros and Cons of a Pushover Analysis of Seismic Performance Evaluation", Engineering Structures, vol.20, 452-464.
- [6] Chopra A.K. and Goel R.K., 2002, "A modal pushover analysis procedure for estimating seismic demands for buildings", Earthquake Engineering & Structural Dynamics, vol.31, 561-582.
- [7] Chopra A.K., Goel R.K, Chintanapakdee C., 2004, "Evaluation of a Modified MPA Procedure Assuming Higher Modes as Elastic to Estimate Seismic Demands", Earthquake Spectra, vol. 20, 757-778.
- [8] Kunnath S.K., 2004, "Identification of modal combinations for nonlinear stati analysis of building structures", Computer Aided Civil and Infrastructure Engineering, 19, 282-295.
- [9] Isakovic T. and Fishinger M., 2006, "Higher modes in simplified inelastic seismic analysis of single column bent viaducts", Earthquake Engineering and Structural Dynamics, vol. 35, 95-114.
- [10] ATC 40, 1996, "Seismic Evaluation and Retrofit of Concrete Buildings: vol. 1", Applied Technology Council, USA.
- [11] ATC 40, 1996), "Seismic Evaluation and Retrofit of Concrete Buildings", Vol. 1", Applied Technology Council, USA.
- [12] FEMA 356, 2000, "Pre-standard and Commentary on the Guidelines for the Seismic Rehabilitation of Buildings", American Society of Civil Engineers, USA.
- [13] IS 1893(Part 1):2002, "Indian Standard Criteria for Earthquake Resistant Design of Structures", Bureau of Indian Standards, New Delhi.
- [14] Luna Ngeljaratan, P. Kamachi and Nagesh R Iyer., 2011, "A critical review on earthquake resistant design provisions of SNI 03-1726-2002 of Indonesia and IS 1893(Part 1)-2002", Journal of Structural Engineering, 38(3), 285-296.
- [15] Ranganathan R., "Reliability Analysis and Design of Structures", Tata McGraw-Hill Publishing Company Limited, New Delhi, 1990.
- [16] "Manual for Seismic Evaluation and Retrofit of Multi-storeyed RC Buildings", IIT, Madras-SERC, Chennai Project Report, Chennai, 2005.
- [17] Oh-Sung Kwon, Amr S. Elnashai., " Probabilistic seismic assessment of structure, foundation, and soil interacting systems", Ph.D Thesis, Department of Civil and Environmental Engineering, University of Illinois, Urbana-Champaign Urbana, Illinois,2007.
- [18] Laura Eads, "Pushover Analysis of 2-Story Moment Frame", From Open Sees Wiki, <http://opensees.berkeley.edu>.
- [19] Dan LUNGU Alexandru ALDEA and Radu VĂCĂREANU "STRUCTURAL RELIABILITY AND RISK ANALYSIS" From Technical University of Civil Engineering of Bucharest.
- [20] Ioana Olteanu1*, Yeudy Felipe Vargas2, Alex-Horia Barbat2, Mihai Budescu1 And Lluís Gonzaga Pujades "VULNERABILITY AND RISK EVALUATION FOR A REINFORCED CONCRETE FRAME" from Universitatea Tehnică „Gheorghe Asachi” din Iași.
- [21] A. Bakhshi*, P. Asadi "Probabilistic evaluation of seismic design parameters of RC frames based on fragility curves" from Department of Civil engineering, Sharif University of Technology, Tehran,